

Laser Diffraction Particle Sizing: Instrument Probe Volume Relocation and Elongation

Robert C. Anderson and Donald R. Buchele
*National Aeronautics and Space Administration
Lewis Research Center
Cleveland, Ohio*

Edward A. Hovenac
*Sverdrup Technology Inc.
NASA Lewis Research Center Group
Cleveland, Ohio*

James A. Lock
*Cleveland State University
Cleveland, Ohio*

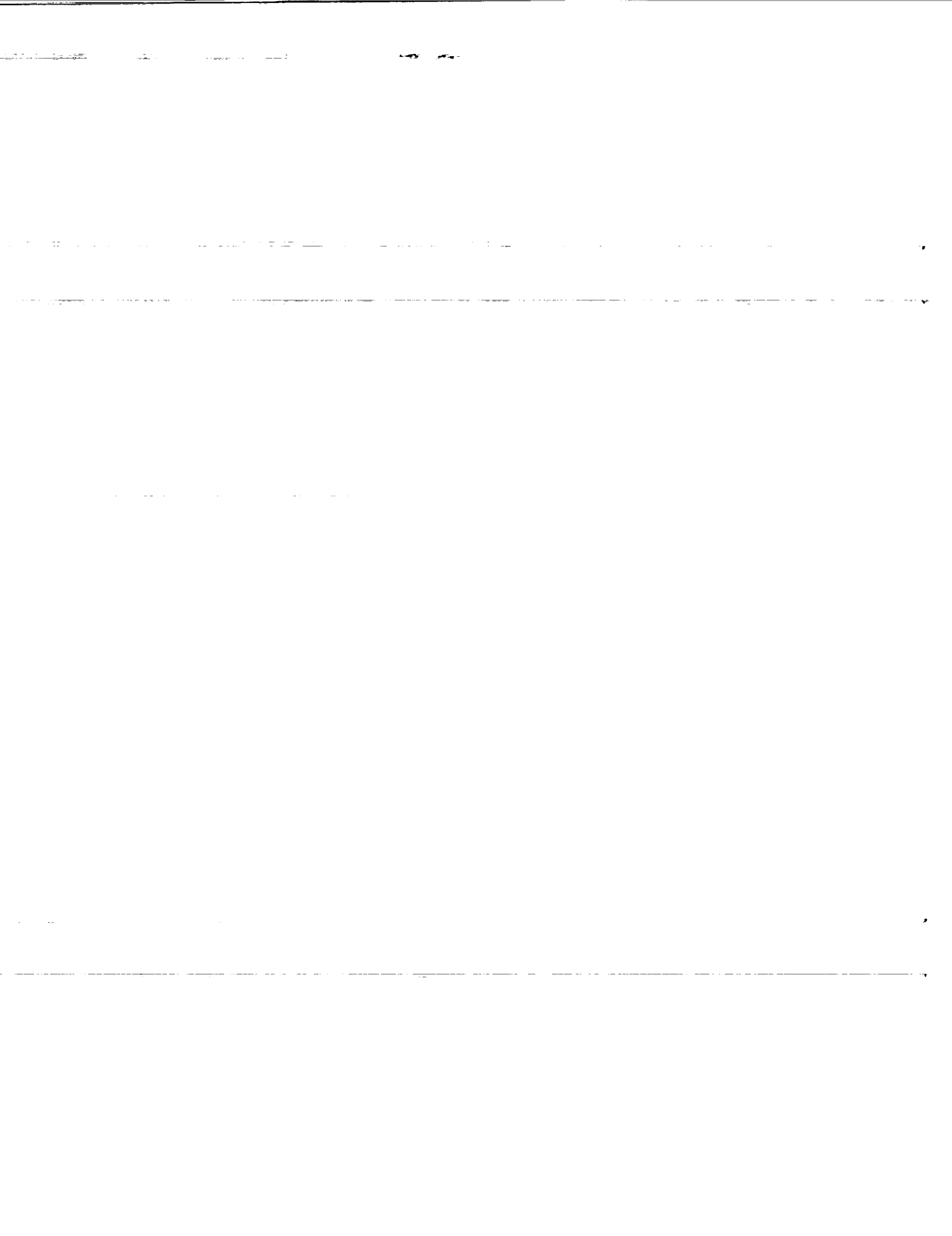
Prepared for the
2nd International Congress on Optical Particle Sizing
sponsored by Arizona State University
Tempe, Arizona, March 5-8, 1990



(NASA-TM-102512) LASER DIFFRACTION PARTICLE
SIZING: INSTRUMENT PROBE VOLUME RELOCATION
AND ELONGATION (NASA) 12 p CSCL 148

N90-18025

Unclas
G3/35 0264814



LASER DIFFRACTION PARTICLE SIZING: INSTRUMENT PROBE VOLUME RELOCATION AND ELONGATION

Robert C. Anderson

NASA Lewis Research Center
Cleveland, Ohio

Donald R. Buchele

NASA Lewis Research Center
Cleveland, Ohio

Edward A. Hovenac

Sverdrup Technology, Inc.
NASA Lewis Research
Center Group
Cleveland, Ohio

James A. Lock

Physics Department
Cleveland State University
Cleveland, Ohio

ABSTRACT

The effective probe volume of laser diffraction particle sizing instruments depends on many instrument parameters. In particular the probe volume axial boundaries and its location along laser beam are essentially defined by the onset of a vignetting effect where light scattered at larger angles from small particles misses the transform lens. This vignetting effect results in a probe volume that must be inconveniently close to the lens in order to detect smaller diameter particles ($< 100 \mu\text{m}$). With the addition of an appropriately designed Keplerian telescope the probe volume may be relocated and elongated. The theory of operation of this supplemental optical system is described. Design considerations for these supplemental optical systems are described including recommendations for lens specifications, assembly and use. An image transfer system is described which has been designed for use on a Malvern 2600HSD instrument. Experimental validation of this image transfer system is described.

INTRODUCTION

Laser diffraction particle sizing instruments are used in aerospace research to characterize fluid sprays in propulsion system experiments and to measure cloud droplet size distributions in aircraft icing research. One problem with the laser diffraction technique is that the transform lens on the detector side of the system must be inconveniently close to the measurement region in order to detect smaller diameter particles ($< 100 \mu\text{m}$). The instrument applicability is thus severely restricted. This problem precludes, for example, using the instrument to measure small particles in tunnels with test section dimensions on the order of 30 cm. where the instrument components must be located outside the tunnel but must measure the droplet distribution in the flow at the center of the tunnel test section.

With the addition of an appropriately designed Keplerian telescope the probe volume may be relocated and elongated. The application of the telescope as an image transfer system is described in the following text.

This system described is designed to allow use of a Malvern 2600HSD Particle Sizer¹ with its lowest range (1.2 to 118 μm .) to sample the aerosol within a small tunnel with a 30 cm. x 30 cm. test section. Theory is developed to show how the additional optics may extend and elongate the probe volume of the instrument to achieve the goal.

Experimental validation of the probe volume enhancement technique is described. Validation was accomplished by comparing measurements using the additional optics with measurements taken without the additional optics. During the validation experiments photomask reticles, latex spheres in water, and water sprays were used to provide input.

INSTRUMENT THEORY OF OPERATION

Introduction and Basic Definitions

For any naturally occurring aerosol such as fogs or the interiors of clouds or for any artificially produced aerosol such as the spray from a nozzle, a descriptive quantity of great interest and importance is the particle size distribution of the aerosol as a function of radius, $n(a)$. If a is the particulate radius, then $n(a)da$ is the number of particles in the aerosol with radii between a and $a+da$. What is typically done in practice is to divide the particle size range into N bins, a given bin beginning with the radius a_j^- and ending with the radius a_j^+ where $1 \leq j \leq N$.² It is often convenient to assign $a_1^- = 0$ and $a_N^+ = \infty$ in order to encompass all possible particle radii. Then the number of particles in particle size bin j is

$$n_j = \int_{a_j^-}^{a_j^+} n(a) da \quad (1)$$

If N_{total} is the total number of particles in the aerosol, then

$$N_{\text{total}} = \int_0^{\infty} n(a) da = \sum_{j=1}^N n_j \quad (2)$$

Diffraction-type particle size analyzers indirectly measure n_j by means of light scattering. That this is possible may be thought of qualitatively in the following way. A large fraction of the power scattered by small particles is scattered into large angles. On the other hand a large fraction of the power scattered by large particles is scattered into the near forward-direction. Thus if one has a set of concentric circular detectors in a plane perpendicular to the axis of the laser beam, the intensity of the light on the outer detector rings will be an indicator of the number of small particles in the aerosol illuminated by the laser beam. The intensity of the light on the inner detector rings will indicate the number of large particles. This qualitative picture, though basically accurate, must be modified somewhat since the small particles also scatter some light onto the inner rings at small scattering angles and the large particles also scatter some light onto the outer rings at larger scattering angles.

Another factor that must be taken into account is the finite size of the laser beam. Each particle scatters the laser light into all scattering angles, θ , according to the Mie scattering formula^{3,4}

$$I_a(\theta) = \frac{I_i k^2 a^4}{4d^2} \left| \mu_a(\theta) \right|^2 \quad (3)$$

where $I_a(\theta)$ is the light intensity scattered into the angle θ from the forward direction, I_i is the incident intensity, d is the distance from the particle of radius a to the observer,

$$k = \frac{2\pi}{\lambda} \quad (4)$$

and

$$\mu_a(\theta) = \frac{2}{(ka)^2} \left[\frac{1}{\sqrt{2}} S_2(\theta) \hat{u}_\theta + \frac{1}{\sqrt{2}} S_1(\theta) \hat{u}_\phi \right] \quad (5)$$

$S_1(\theta)$ and $S_2(\theta)$ are the usual complex Mie scattering amplitudes and the factors of $1/\sqrt{2}$ multiplying them result from the assumption of an unpolarized laser beam. The factors \hat{u}_θ and \hat{u}_ϕ are unit vectors in the spherical coordinate system. The quantity $\mu_a(\theta)$ satisfies the normalization condition

$$\lim_{\theta \rightarrow 0} \lim_{a \rightarrow \infty} \mu_a(\theta) = 1 \quad (6)$$

Finally, equation (3) assumes that the measurement is made in the far field, comparable to the Fraunhofer limit for diffraction where $d > (8a^2/\lambda)$. To insure that all light scattered in a given direction goes to the same point on the detector array regardless of the particle's location in the laser beam a lens is inserted one focal length from the detector.

The purpose of the lens can be understood in the following way. The rays of light leaving each of the particles in the θ, ϕ direction are all parallel. These parallel rays are incident on the lens and are focused by it to a point on the focal plane in much the same way that the parallel rays describing a plane wave would be focused.

Although many particle sizers measure one particle at a time, the diffraction-type particle sizer operates so as to measure the sizes of all the particles at once. This is possible since the scattered electric fields from all of the particles differ from each other by only a position dependent phase factor. When the fields are combined to form the total intensity, the sum over the phase is an incoherent one (even for coherent incident laser light) and the resultant intensities, rather than the fields, are additive. We then obtain for the scattered light intensity at angle θ

$$I_{\text{total}}(\theta) = \int_0^{\infty} n(a) I_a(\theta) da = \sum_{j=1}^N \int_{a_j^-}^{a_j^+} n(a) I_a(\theta) da \quad (7)$$

As a final introductory note about these diffraction instrument principles of operation, it is well known that the light scattered by large radius particles in the near-forward direction approaches the pattern of light diffracted by apertures or obstacles of the same radius.⁵ Since the pattern of diffracted light is the most significant component for the instruments of interest here, the light intensity, analogous to equation (3), resulting from Fraunhofer diffraction by apertures or obstacles of radius a is^{3,4}

$$I_a(\theta) = \frac{I_i k^2 a^4}{4d^2} \left[\frac{2J_1(ka\theta)}{(ka\theta)} \right]^2 \quad (8)$$

Again we have the normalization condition

$$\lim_{\theta \rightarrow 0} \frac{2J_1(ka\theta)}{(ka\theta)} = 1 \quad (9)$$

The Light Intensity on the Detector Array and the T- Matrix

Consider the situation of Figure 1 where a plane wave of light with electric field E_i is incident either on an aperture of radius a or on a particle of radius a . The scattered light travels a distance d to the lens of radius A and focal length f . The light travels through the lens and then an additional distance f to the detector array. A point on the detector array has the coordinate r_o and makes an angle θ_o with the axis of symmetry.

According to the wave optics formalism for image formation from lenses, (i) light waves leaving an object travel in all directions. (ii) The amplitude and phase of the light waves distort according to Fresnel diffraction between optical elements. Mathematically in going a distance d between two arbitrary planes called 1 and 2, $E(r_1)$ becomes distorted to

$$E(r_2) = \int d^2r_1 E(r_1) \left[\frac{-ik}{2\pi d} \right] e^{ikd} e^{\frac{ik(r_1-r_2)^2}{2d}} \quad (10)$$

(iii) The amplitude and phase of light waves distort in going through a lens.

$E(r)$ becomes

$$Ap_A(r) e^{-ikr^2/2f} E(r) \text{ where}$$

$$Ap_A(r) = 1 \text{ if } r \leq A \text{ or } 0 \text{ if } r > A$$

and A is the lens radius. This formalism may be used to propagate either the diffracted or scattered field through the lens to the detector array.

Consider first the case of diffraction from an aperture. If

$$\frac{A^2}{\lambda d} \geq .125 \text{ and } r_o \leq (A-a) \frac{f}{d} \quad (11)$$

then the intensity on the detector array is given by equation (8). The scattering angle θ is equal to the detector array angle θ_o .

Consider circularly symmetric detector rings, the i^{th} of which starts at the radius r_i^- from the center of the array and ends at the radius r_i^+ .

The power incident on ring i is given by

$$\begin{aligned} P_{\text{ring } i} &= \int_{r_i^-}^{r_i^+} r_o dr_o \int_0^{2\pi} d\phi_o I_o(\theta) \\ &= I_i \frac{\pi k^2 a^4}{2f^2} \int_{\theta_i^-}^{\theta_i^+} \theta_o d\theta_o \left[\frac{2J_1(ka\theta_o)}{(ka\theta_o)} \right] \quad \text{where } \theta_i^\pm \approx \frac{r_i^\pm}{f} \end{aligned} \quad (12)$$

For this case, power deposited onto ring i by the entire particle size distribution is

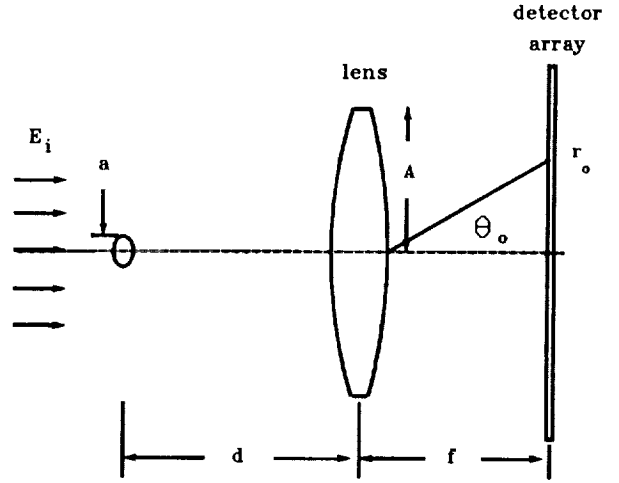
$$P_i^{\text{total}} = I_i \sum_{j=1}^N T_{ij} W_j \quad (13)$$

where T_{ij} is the fraction of power deposited in the i^{th} ring by a unit weight of particles in the j^{th} size bin. W_j is the weight of particles in the j^{th} size bin.

Particulate Weights From the Experimentally Measured Power

The Malvern instrument contains 30 concentric detector rings which produce 30 experimentally measured scattered or diffracted light powers, P_i . If one were considering Fraunhofer diffraction, the detector power P_i at \hat{r}_o is

Figure 1 Schematic of Laser Diffraction Measurement System



maximized by

$$\frac{dP_i}{d\theta_0} = 0 = \frac{d}{d\theta_0} \left[\frac{J_1^2(ka\theta_0)}{(ka\theta_0)} \right] \quad (14)$$

or

$$ka\theta_0 = \frac{2\pi ar_0}{\lambda f} = 1.357. \quad (15)$$

Thus if we wish to define the particle size bin boundaries so that each size bin diffracts light primarily to a single detector ring, then we have

$$\begin{aligned} a_1^+ &= \infty \\ a_i^- &= \frac{1.357\lambda f}{2\pi r_i^+} \quad \text{for } 1 \leq i \leq 29 \\ a_{i+1}^+ &= a_i^- \quad \text{for } 1 \leq i \leq 29 \\ a_{30}^- &= 0 \end{aligned} \quad (16)$$

Notice that these definitions provide 30 particle size bins for the 30 experimental detector signals and we obtain

$$P_i = \sum_{j=1}^{30} T_{ij} W_j \quad \text{for } 1 \leq i \leq 30 \quad (17)$$

This can now be considered as a set of 30 equations in the 30 unknowns W_j and can be directly solved for the W_j via the inversion

$$W_j = \sum_{i=1}^{30} (T^{-1})_{ji} P_i \quad (18)$$

However, the determination of the W_j in practice is difficult since the T -matrix is almost always ill-conditioned. Ill-conditioned may be described as follows. One never knows the P_i exactly since the experimentally observed P_i are the true P_i produced by the particle size distribution plus or minus a little noise or error. If we measured the P_i 10 different times, we would expect to obtain 10 slightly different answers. If we put these slightly different P_i into equation (18) we would expect to obtain slightly different sets of W_j . In equations like equation (18), we expect that slight perturbations in the cause, P_i , produces slight perturbations in the effect W_j . This is true so long as the matrix T is well conditioned, i.e. $\det(T) \approx 1$. If however $\det(T) \gg 1$ or $\det(T) \ll 1$, the matrix T is ill-conditioned. As a result small perturbations in the cause can produce dramatically large changes in the effect. For our situation, small changes in the P_i due to optical noise or experimental error can lead to catastrophic changes in the W_j obtained by equation (18).

In spite of this, physically meaningful weights W_j may still be obtained because of a constraint on the system. Negative values of W_j are not physically meaningful; we must have $W_j \geq 0$. If the set of W_j obtained from equation (18) possesses a number of negative components (which is usually the case) a suitable iterative procedure allows us to find the closest physically meaningful W_j to it.

The Malvern Particle Sizer and Vignetting

Consider the Malvern geometry of Figure 2. A laser beam of radius B illuminates a chamber containing the aerosol of interest. The chamber begins a distance d_1 from the Malvern lens of radius A and it ends a distance d_2 from the lens. A point on the detector array is a distance r_0 from the Malvern axis. Particles within the chamber scatter light at all angles θ . The light scattered at small angles is collected on the inner detector rings and the light scattered at larger angles is collected on the outer detector rings. To get to the detector the light must pass through the lens. If a particle is sufficiently far away from the lens, the light it scatters at the angle θ will be outside the limit rays $\alpha\alpha'$ and $\beta\beta'$ of Figure 2 and it will miss the lens and thus not make it to the detector array. This is known as vignetting. As the radial distance from center on the detector plane r_0 increases, the detector at that position will be less likely to receive the light scattered from distant aerosol particles. This presents a potential problem for the Malvern operation since if vignetting occurs, the outer rings record the power from fewer particles than the inner rings do. This introduces an artificial bias into the P_i data since we always previously assumed that the light scattered from all the particles in the aerosol was received by all the detectors.

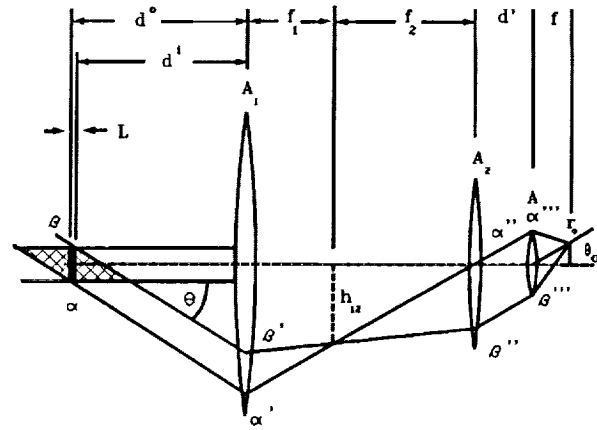
From geometrical considerations, vignetting is avoided at r_0 if

$$\frac{r_0}{f} = \tan \theta \quad (19)$$

Thus for example if $f=100\text{mm.}$, $f_1=246\text{ mm.}$, and $f_2=390\text{ mm.}$, one would employ the $F=63\text{mm.}$ T-matrix for such a system.

The vignetting geometry for this three-lens system is different than the vignetting geometry of the single lens system. The vignetting geometry for the multiple lens situation is shown in Figure 4. The first lens (on the left in Figure 4) has radius A_1 , and focal length f_1 ; the second lens has radius A_2 and focal length f_2 ; and the Malvern lens has radius A and focal length f . Lenses 1 and 2 form a Keplerian telescope with a magnification $\theta_o/\theta = f_1/f_2$. As shown by the two rays, the Malvern lens diameter is focussed into the test section at a distance $(d^o+d^i)/2$ from the first lens. When this image has a larger diameter than the laser beam, it creates a distance $L = |d^o-d^i|$, shown in black in Figure 4, that is the totally unvignetted length for scattering angle θ . The shaded area in Figure 4 represents a partially vignetted volume which becomes important as experimental results are analyzed in a later section.

Figure 4 Vignetting Diagram for 3-Lens System.



The light that scatters at an angle θ between the limit rays $\alpha\alpha'$ and $\beta\beta'$ will go through the first lens between α' and β' , go through the second lens between α'' and β'' , go through the Malvern lens between its top at α''' and its bottom β''' and be focused to the point r_o on the detector array at a detector angle θ_o . We wish to find the distance d^o and d^i where these limit rays cross the laser beam in order to define the no-vignetting boundaries. Consider first the ray $\alpha\alpha'\alpha''\alpha'''\alpha'''\alpha''\alpha''\alpha'$. We have, measuring positive distances in the downward direction,

$$\alpha''' = -A \quad (25)$$

$$\alpha'' = d' \tan \theta_o - A \quad (26)$$

$$h_{12} = f_2 \tan \theta_o = f_1 \tan \theta \quad (27)$$

$$\alpha' = h_{12} + \frac{h_{12} - \alpha''}{f_2} f_1 \quad (28)$$

and

$$\frac{(\alpha' - B)}{d^o} = \tan \theta \quad (29)$$

These may be combined to give

$$d^o = \frac{f_1(f_1+f_2)}{f_2} - \frac{d' f_1^2}{f_2^2} + \frac{f f_1}{f_2 r_o} \left[\frac{A f_1}{f_2} - B \right] \quad (30)$$

and

$$\alpha' = (f_1+f_2) \frac{r_o}{f} - \frac{d' r_o f_1}{f_2 f} + \frac{A f_1}{f_2} \quad (31)$$

Similarly for the ray $\beta\beta'\beta''\beta'''\beta'''\beta''\beta''\beta'$ we have

$$\beta''' = A \quad (32)$$

$$\beta'' = d' \tan \theta_o + A \quad (33)$$

$$\beta' = h_{12} + \frac{h_{12} - \beta''}{f_2} f_1 \quad (34)$$

and

$$\frac{(\beta' + B)}{d^i} = \tan \theta \quad (35)$$

These may be combined to give

$$d^i = \frac{f_1(f_1+f_2)}{f_2} - \frac{d'f_1^2}{f_2^2} - \frac{ff_1}{f_2r_o} \left[\frac{Af_1}{f_2} - B \right] \quad (36)$$

and

$$\beta'' = d' \frac{r_o}{f} + A \quad (37)$$

We wish the limit rays to be determined by the size of the standard Malvern lens, and have no further vignetting be created by lenses 1 and 2. Thus we must require the radii of these added lenses to be

$$A_2 \geq \beta'' = \frac{d'r_o}{f} + A \quad (38)$$

$$A_1 \geq \alpha' = (f_1+f_2)\frac{r_o}{f} + \frac{f_1}{f_2} \left[A - \frac{d'r_o}{f} \right] \quad (39)$$

Consider the following parameters for an example 3-lens system

$$f = 100 \text{ mm. } f_2 = 390 \text{ mm. } f_1 = 246 \text{ mm.}$$

$$A = 22.5 \text{ mm. } A_2 = 57 \text{ mm. } A_1 = 92 \text{ mm.}$$

$$d' = 145 \text{ mm. and } r_o = 14.3 \text{ mm.}$$

Then equation (38) yields $57 \geq 42$ and equation (39) yields $92 \geq 92$ so no additional vignetting is expected from lenses 1 and 2 in this system.

Consider the situation of vignetting. Assume that the aerosol chamber of interest is of length L . For a given r_o , the center of the measurement volume is at

$$\frac{d^o+d^i}{2} = \frac{f_1}{f_2} \left[f_1 + f_2 - d' \frac{f_1}{f_2} \right] \quad (40)$$

This is independent of r_o . So if the center of the aerosol chamber is placed at the distance

$$D = \frac{f_1}{f_2} \left[f_1 + f_2 - d' \frac{f_1}{f_2} \right] \quad (41)$$

from the first lens, it is exactly centered with respect to the limit rays, no matter what their angular inclination is. If $L \leq |d^o-d^i|$ or

$$r_o \leq \frac{2ff_1}{f_2L} \left[\frac{Af_1}{f_2} - B \right] \quad (42)$$

then the aerosol chamber fits entirely within the cylindrical region within the limit rays, and the detector rings see light scattered from all the particles.

The three-lens case represents an interesting improvement over the standard Malvern one-lens configuration for short focal length lenses. Consider for example the case of $f = 63$ mm. with $A = 17.5$ mm., Equation (21) shows that the longest chamber with no vignetting is 55 mm. assuming the laser beam radius B is 4.5 mm. and $r_o = 14.3$ mm. for the outermost edge of the last detector ring.⁶ Even this length would be impractical especially if the Malvern instrument components are to be located outside the walls of a tunnel test section since it assumes that the chamber begins at the position of the Malvern lens.

On the other hand, the three-lens system allows the chamber to be longer, 83 mm. for the effective 63 mm. focal length system of the above example. This system also allows the probe volume to be located far from the first lens; equation (41) yields 345 mm. for the system in the above example. This allows non-vignetted measurements to be made from within a test chamber located far enough away from the first lens to allow room for tunnel walls and windows.

EXPERIMENTAL VALIDATION OF AN IMAGE TRANSFER LENS SYSTEM

A Transfer lens system has been assembled, and validated at the NASA Lewis Research Center with a Malvern 2600 HSD instrument. Table 1 gives the specifications for the optical system using the nomenclature of Figure 4.

This lens system was designed to enable use of the Malvern Instrument with its lowest range in a tunnel with a 30 cm. x 30 cm. cross-section. The goal was to center the non-vignetted section within the 30 cm. width of the tunnel allowing about 10 cm. for the tunnel walls and windows.

TABLE 1 - NASA Lewis Image Transfer System Specification

Lens	Surface Number	Clear Aperture	Radius of Curvature	Thickness (on axis)	Material (to the right of the surface)
A ₁ (3-element, airspace)	1	175 mm.	∞	20.5 mm.	Glass
	2	175 mm.	-279 mm.	9.5 mm.	Air
	3	175 mm.	∞	14.0 mm.	Glass
	4	175 mm.	-423 mm.	9.5 mm.	Air
	5	175 mm.	423 mm.	14.0 mm.	Glass
	6	175 mm.	∞		
A ₂ (1-element)	1	115 mm.	203 mm.	14.0 mm.	Glass
	2	115 mm.	∞		

Lens A₁ Computed Effective focal length = 240 mm.
 Lens A₂ Computed Effective focal length = 394 mm.

General specifications

- Glass - Borosilicate crown glass
- Surface pitch - 80-50 scratch and dig
- 40-30 scratch and dig within 6.5 mm radius of the optical axis
- Surface coating - for minimum reflectance at He-Ne laser wavelength 0.6238 nm.

Several items in the specification take on particular importance when the system is used with a diffraction particle sizing instrument. Lens imperfections must be avoided in the area around the optical axis where the unscattered laser beam passes through in order to minimize background noise. The more stringent surface finish specifications in that area are therefore important. Antireflection coating flaws in the central area should also be avoided. Great care must be exercised when assembling the lens system to avoid marring the coating or scratching the lens in this central area. Antireflection coating is also very important in this application because the Malvern system is sensitive to reflections and the added lenses have increased the number of optical surfaces from 2 to 10 when the surfaces of the multi-element lens are counted.

Several methods were used to characterize the performance of the transfer lens system. The vignetting limits for the outer detector rings were measured and validation measurements were made using photomask reticles, monodisperse latex spheres in water, and a water spray.

Figure 5 shows the response of the outer three Malvern detector rings (with the 3-lens system) as a diffuse scattering medium was moved along the laser beam axis from 20 to 36 centimeters measured from the first optical surface of A₁. The plot indicates a beam segment between 24 and 33 centimeters where there is no appreciable fall off in the signal in the outer ring. This is the length over which we would expect no vignetting effects.

The data shown in Figure 6 gives the response of the Malvern system with and without the transfer lens system for two different photomask reticles⁷ placed at various distances from the first optical surface. The expected result is a Median Volume Diameter (MVD) or D(50%) of 50 micrometers. All the data for the case without the transfer lens system were taken with the photomask reticle located 63 mm. from the single detector lens surface. The effects of vignetting can be easily seen in the data taken with the transfer system in place; those data points at about 50 micrometers indicated locations where there is no vignetting effect. The effective usable beam length for these reticles (where the measured value of D(50%) is about 50 micrometers) ranges from about 110 mm. to 350 mm. as measured from the first detector lens surface with a center at 230 mm. This usable range is longer than that predicted because there is a relatively small weight in the small diameter size bins for these reticles. It is therefore reasonable to expect that the data will be good over the partially vignetted beam length as shown in the shaded area in Figure 4.

Using the data from Table 1 and assuming d' = 150 mm., r_o = 14.3 mm., and A = 22 mm. equation (41) yields a value of D = 330 mm. and from equations (30) and (36) the length of the totally non-vignetted beam segment, L = 76 mm. Note that the value of D is the distance from the first principal plane of lens A₁ which is 27 mm. from the first optical surface inside the lens. For valid comparison D_{effective} = D - 27 = 303 mm. should be used in the discussion of the validation experiment results. This falls within the non-vignetting range determined in Figure 5 and within the useable range determined in Figure 6. The predicted non-vignetted length is 76 mm. The predicted non-vignetted range thus extends from 265 mm. to 341 mm. which falls almost fully within the measured non-vignetted range. It is easily seen in equation (41) that the value of D depends only on the focal lengths of A₁ and

Figure 5 Vignetting on the Outer 3 Malvern Detector Rings Using Diffuse Scatterer.

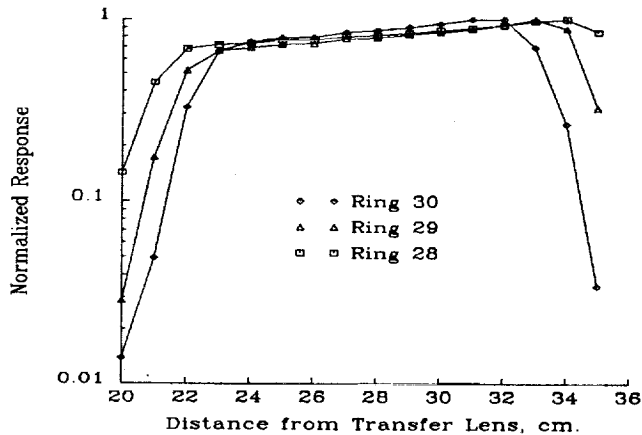
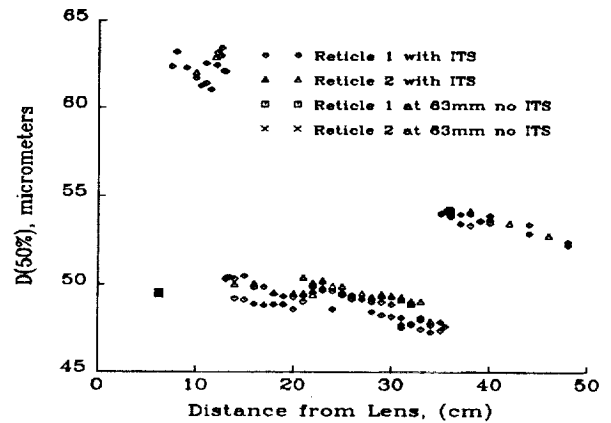


Figure 6 Photomask Reticle Response for Malvern With and Without Image Transfer System.



A_2 and the value of d' . In the validation experiments there was a relatively large uncertainty in the measured value of d' . Since both the diffuse scatterer and reticle experiments indicate similar non-vignetted lengths, it is assumed that an error in the value of d' caused the predicted value of D to be shifted up.

The transfer lens system was also validated using monodisperse latex spheres suspended within a flow cell filled with water and located 300 mm. from the first optical surface. Figure 7 shows the results of these tests. Several data points were taken using a different monodisperse latex sphere distribution for each. The peak diameter measured is plotted versus the known size. The difference is small as it should be.

The transfer lens system was further tested in a water spray. Figure 8 shows data taken both with and without the transfer lens system in place. An air-assisted atomizer was used to produce a repeatable water spray. Ideally, at a given nozzle air pressure the data points should fall on top of each other. There is about 1 micrometer variation in the value of $D(50\%)$ or the Median Volume Diameter (MVD) at nozzle pressures where there is maximum scatter. There appears to be no obvious trend in the difference between the case with and the case without the transfer lens system. That is, the transfer lens system doesn't introduce any systematic error into the measurement.

Figure 7 Test of Malvern Image Transfer system Using Monodisperse Latex Spheres in Water 300 mm. from Lens.

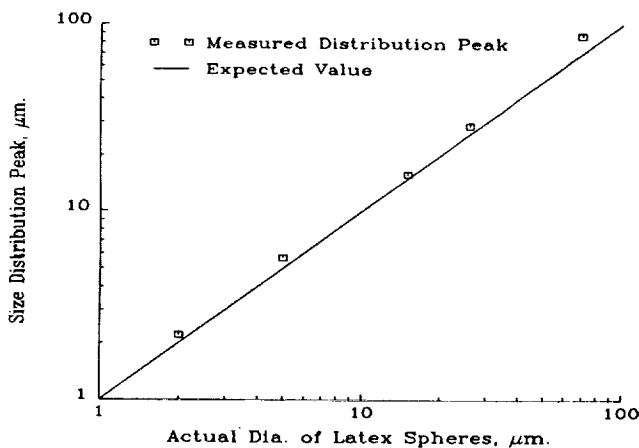
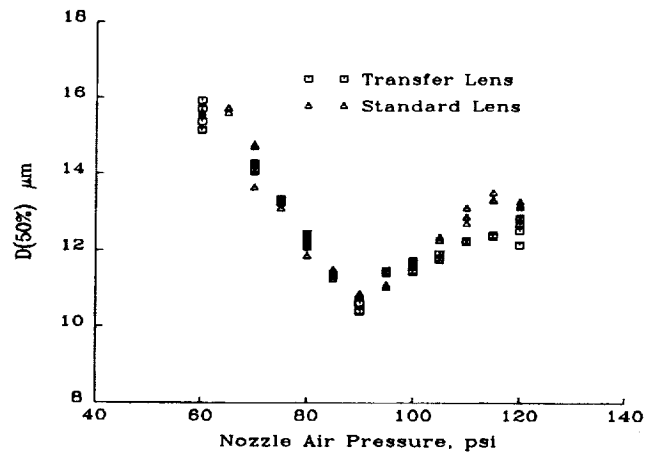


Figure 8 Malvern Results With and Without the Image Transfer System Measuring Water Spray from Air-assisted Atomizer.



SUMMARY AND CONCLUDING REMARKS

The previous text has described the theory of operation of laser diffraction particle sizing instruments and has described the analysis and design of an optical system which can relocate and enlarge the usable beam length (segment of the laser beam along which there are no vignetting effects). It has been shown that with a specific system designed at the NASA Lewis Research Center for a Malvern 2600HSD, the usable beam length has been relocated to 230 mm. instead of 55 mm. and its length has been increased to 76 mm. instead of 55 mm.

The operation of the lens system has been tested with a photomask reticle, with latex spheres in water, and with a water spray. Results with and without the lens system compare favorably.

The lens system gives laser diffraction instruments a capability not available before with the lower size range. The aerosol can be located far from the optical surfaces to prevent accumulation on the surfaces of light scattering droplets.

REFERENCES

1. Malvern Instruments, Ltd., Malvern, Worcestershire, England.
2. J. Swithenbank, J. Beer, D. S. Taylor, D. Abbot, and C.G. McCreath, "A Laser Diagnostic Technique for the Measurement of Droplet and Particle Size Distribution," *Experimental Diagnostics in Gas Phase Combustion Systems*, B. T. Zinn, Ed., Vol. 53, of Progress in Aeronautics and Astronautics, AIAA, 1977, pp. 421-447.
3. H. C. Van de Hulst, *Light Scattering by Small Particles*, (Dover Publications, Inc., 1981).
4. Kerker, *The Scattering of Light* (Academic Press, 1969).
5. M. Born and E. Wolf, *Principles of Optics*, Sixth Ed. (Pergamon Press, 1989).
6. L. G. Dodge, "Calibration of the Malvern particle sizer," *Appl. Opt.* 14, 2415 (1984).
7. Reticles sold through Laser-Electro-Optics Ltd., Tempe, Ariz.

1. Report No. NASA TM-102512		2. Government Accession No.		3. Recipient's Catalog No.	
4. Title and Subtitle Laser Diffraction Particle Sizing: Instrument Probe Volume Relocation and Elongation				5. Report Date	
				6. Performing Organization Code	
7. Author(s) Robert C. Anderson, Donald R. Buchele, Edward A. Hovenac, and James A. Lock				8. Performing Organization Report No. E-5315	
				10. Work Unit No. 505-62-01	
9. Performing Organization Name and Address National Aeronautics and Space Administration Lewis Research Center Cleveland, Ohio 44135-3191				11. Contract or Grant No.	
				13. Type of Report and Period Covered Technical Memorandum	
				14. Sponsoring Agency Code	
12. Sponsoring Agency Name and Address National Aeronautics and Space Administration Washington, D.C. 20546-0001					
15. Supplementary Notes Prepared for the 2nd International Congress on Optical Particle Sizing, sponsored by Arizona State University, Tempe, Arizona, March 5-8, 1990. Robert C. Anderson and Donald R. Buchele, NASA Lewis Research Center. Edward A. Hovenac, Sverdrup Technology, Inc., NASA Lewis Research Center Group, Cleveland, Ohio 44135. James A. Lock, Physics Dept., Cleveland State University, Cleveland, Ohio 44115.					
16. Abstract The effective probe volume of laser diffraction particle sizing instruments depends on many instrument parameters. In particular the probe volume axial boundaries and its location along laser beam are essentially defined by the onset of a vignetting effect where light scattered at larger angles from small particles misses the transform lens. This vignetting effect results in a probe volume that must be inconveniently close to the lens in order to detect smaller diameter particles ($< 100 \mu\text{m}$). With the addition of an appropriately designed Keplerian telescope the probe volume may be relocated and elongated. The theory of operation of this supplemental optical system is described. Design considerations for these supplemental optical systems are described including recommendations for lens specifications, assembly and use. An image transfer system is described which has been designed for use on a Malvern 2600HSD instrument. Experimental validation of this image transfer system is described.					
17. Key Words (Suggested by Author(s)) Particle sizing Optics Measurements			18. Distribution Statement Unclassified - Unlimited Subject Category 35		
19. Security Classif. (of this report) Unclassified		20. Security Classif. (of this page) Unclassified		21. No. of pages 12	22. Price* A03

